Am J Physiol Heart Circ Physiol 289: H792–H800, 2005.
First published April 15, 2005; doi:10.1152/ajpheart.00050.2005.

Contribution of Na^+-K^+ pump and K_{IR} currents to extracellular pH-dependent changes of contractility in rat superior mesenteric artery

Moon Young Kim,[1] Guo Hua Liang,[1] Ji Aee Kim,[1] Seong Hoon Park,[2] Jong Sik Hah,[1] and Suk Hyo Suh[1]

[1]*Department of Physiology and Medical Research Institute and* [2]*Department of Internal Medicine, College of Medicine, Ewha Women's University, Seoul, Republic of Korea*

Submitted 18 January 2005; accepted in final form 13 April 2005

Kim, Moon Young, Guo Hua Liang, Ji Aee Kim, Seong Hoon Park, Jong Sik Hah, and Suk Hyo Suh. Contribution of Na^+-K^+ pump and K_{IR} currents to extracellular pH-dependent changes of contractility in rat superior mesenteric artery. *Am J Physiol Heart Circ Physiol* 289: H792–H800, 2005. First published April 15, 2005; doi:10.1152/ajpheart.00050.2005.—We compared the branches and trunk of rat superior mesenteric artery (SMA) with respect to extracellular pH (pH_o)-dependent changes in vascular contractility. Decreases in pH_o from 7.8 to 6.4 significantly reduced apparent affinity (pD_2) to norepinephrine (NE) and maximal contraction by NE, which were more prominent in larger-diameter arteries. On the other hand, decreases in pH_o significantly reduced Ba^{2+}-sensitive K^+-induced relaxation (which was evoked by elevation of extracellular K^+ concentration from 6 to 12 mM) in the first branch and inhibited inwardly rectifying K^+ (K_{IR}) currents in cultured smooth muscle cells (SMCs) of SMA. RT-PCR revealed transcripts for Kir2.1 in the SMCs. Real-time PCR analysis revealed 6.1-, 3.3-, and 2.2-fold increases in the Kir2.1 mRNA-to-β-actin mRNA ratios of SMCs of the third, second, and first branches, respectively, vs. the corresponding relative levels of trunk SMCs. The magnitudes of K^+-induced relaxation were significantly greater in smaller-diameter arteries, and there was a strong correlation between the transcript levels of Kir2.1 and K^+-induced relaxation. A decrease in pH_o reduced ouabain-sensitive K^+-induced relaxation and ouabain-induced contraction. A decrease in pH_o from 7.4 to 6.4 depolarized membrane potential of the cultured SMCs. From these results, we conclude that an increase in pH_o activates K_{IR} currents and the Na^+-K^+ pump, which then reduces vascular contractility. Inasmuch as K_{IR} channel densities are significantly greater in smaller-diameter arteries, the reduction in vascular contractility on increasing pH_o is more pronounced in smaller-diameter arteries.

inwardly rectifying K^+ current; vascular contractility; potassium channels; smooth muscle cells

THE CHANGES IN EXTRACELLULAR and intracellular pH (pH_o and pH_i, respectively) have been shown to modulate vascular contractility by affecting the activities of ion channels and pumps (1). H^+ may interact with voltage-operated Ca^{2+} (VOC) channels both internally and externally (6, 7). In bovine pial and porcine coronary arteries, an increase in pH_i potentiated the Ca^{2+} currents through L-type channels (6, 7). In addition, acidosis activated Ca^{2+}-activated K^+ channels in porcine coronary artery smooth muscle cells (SMCs; Ref. 4) and ATP-sensitive K^+ channels in rat cerebellar arterioles (5). These effects of H^+ on Ca^{2+} and K^+ channels could clearly account for the decrease in intracellular Ca^{2+} concentration and also for the decrease in contractility on acidification. On the other hand, decreases in pH_i and pH_o inhibited inwardly rectifying K^+ (K_{IR}) currents (10, 20, 22). K_{IR} current activation would be expected to lead to hyperpolarization, and hence, vasorelaxation. It has been suggested that K_{IR} channels are expressed at higher densities in small-diameter arteries (15). In porcine coronary artery, current densities were greater in cells isolated from smaller-diameter arteries. In contrast, arterial diameter was found to have little effect on the densities of voltage-dependent K^+ currents (15). These results suggest that the modulation of vascular contractility by H^+ varies depending on arterial diameter.

The present study was undertaken to elucidate the effect of arterial diameter on H^+-induced vascular contractility. We provide evidence for activation of the Na^+-K^+ pump and K_{IR} currents by extracellular alkalinization.

METHODS

The animals used in this study were treated in accordance with the National Institutes of Health *Guide for the Care and Use of Laboratory Animals* (NIH Publication No. 85-23, Revised 1996), and the experimental and animal care protocol was approved by the Animal Care and Use Committee of the Ewha Women's University. All experiments were performed at 37°C.

Dissection of superior mesenteric arteries. Sprague-Dawley rats (5–6 mo of age) of either gender were anesthetized by injection of pentobarbital sodium (150 mg/kg body wt ip) and killed by exsanguination. Superior mesenteric arteries (SMAs) were dissected out and divided into four regions including the trunk and the first, second, and third branches. An expanded explanation of SMA branches and trunk is available in an online supplement at http://ajpheart.physiology.org/cgi/content/full/00050.2005/DC1. When the second branch was long enough, its distal portion was included in the third branch, inasmuch as the third branch was relatively short.

Contraction measurement on isolated arterial rings. A home-made myograph was used to record mechanical responses from the arterial ring segments (2.0–3.0 mm) from each region. An expanded explanation of the myograph and the technique used to mount the rings is available in the online supplement. The rings of the trunk and branches were threaded with two strands of stainless steel wire (trunk, 100 μm diameter; branches, 40 μm diameter); one was anchored in the organ bath chamber (1 ml), and the other was connected to a mechanotransducer (model FT-03; Grass). The chamber was perfused at a flow rate of 2.5 ml/min with oxygenated (95% O_2-5% CO_2) Krebs-Ringer bicarbonate solution using a peristaltic pump. The

Address for reprint requests and other correspondence: S. H. Suh, Dept. of Physiology, College of Medicine, Ewha Women's Univ., 911-1 Mok-6-dong, Yang Chun-gu, Seoul, Republic of Korea, 158-710 (E-mail: shsuh@ewha.ac.kr).

The costs of publication of this article were defrayed in part by the payment of page charges. The article must therefore be hereby marked "*advertisement*" in accordance with 18 U.S.C. Section 1734 solely to indicate this fact.

composition (in mM) of the Krebs buffer was 118.3 NaCl, 4.7 KCl, 1.2 $MgCl_2$, 1.22 KH_2PO_4, 2.5 $CaCl_2$, 25.0 $NaHCO_3$, and 11.1 glucose, pH 7.4. The pH of the solution was changed by changing the HCO_3^- concentration. In experiments to examine the effects of pH_o on K^+-induced relaxation, oxygenated (100% O_2) HEPES-buffered solution was also used. The composition (in mM) of HEPES-buffered solution was 150 NaCl, 6 KCl, 1.5 $CaCl_2$, 1 $MgCl_2$, 10 HEPES, and 10 glucose, pH 7.4.

To abolish the influence of endothelium on contraction, endothelium was damaged by passing air through the lumen of the vessel (17) and pretreating the vessel with 30 μM N^G-nitro-L-arginine methyl ester (L-NAME). Optimal resting tension (0.5–1 g) was applied. Rings were contracted with norepinephrine (NE). When the contraction reached a steady state, extracellular K^+ concentration ($[K^+]_o$) was increased from 6 to 12 mM to evoke K^+-induced relaxation.

Rat SMA SMC culture. Vascular SMCs were isolated using a previously described procedure (16). Briefly, intact arteries were placed in a Ca^{2+}-free extracellular solution that contained (in mg/ml) 1 papain, 1 bovine serum albumin, and 1 dithioerythritol and were incubated for 4–6 min at 37°C. Samples were then washed several times with ice-cold Ca^{2+}-free solution and incubated in a digestive solution [in which 1 mg/ml collagenase (Wako), 1 mg/ml bovine serum albumin, and 1 mg/ml dithioerythritol were contained in Ca^{2+}-free solution] (5 min for third and second branches, 10 min for first branch, and 15 min for trunk) at 37°C. The tissues were then washed several times with ice-cold extracellular solution to remove any enzymes and were agitated with a fire-polished Pasteur pipette to yield single SMCs.

Cells were grown in growth medium (100 ml) composed of 86 ml of DMEM, 10 ml of fetal bovine serum, 2 ml of penicillin-streptomycin (100 U/ml final), 1 ml of L-glutamine, and 1 ml of minimal essential amino acids. Cells were passaged and used up to the fifth passage for functional studies. To identify the nature of the cells, we used immunohistochemical techniques to detect smooth muscle α-actin (data not shown).

Cell cultures were maintained at 37°C in fully humidified air with a 5% CO_2 atmosphere. Cells were detached by exposure to trypsin, reseeded on gelatin-coated coverslips, and maintained in culture for 2–4 days before use. Measurements were performed on nonconfluent cells.

RT-PCR. Total RNA was extracted from cultured SMCs that were prepared using TRIzol reagent (Molecular Research Center; Cincinnati, OH) following the manufacturer's instructions. First-strand cDNA was generated from total RNA using BcaBEST polymerase (Takara Shuzo). The Kir2.1 primers were 5′-ACCGCTACAGCATCGTCTCT-3′ (sense) and 5′-GTCTTTCTTCACAAAGCGGC-3′ (antisense). The size of the expected fragment was 139 bp. PCR reactions were performed using Bca-optimized *Taq* polymerase (Takara Shuzo). The PCR conditionings used were as follows: initial denaturation for 1 min at 94°C, 35 amplification cycles (1 min at 94°C, 1.5 min at 55°C, and 1.5 min at 72°C for each cycle), a final extension of 10 min at 72°C, and rapid cooling to 4°C. PCR products were visualized on 1% agarose gel using a 100-bp DNA ladder marker (New England BioLabs; Beverly, MA) as a standard.

RT reaction. RNA (5 μg) was used for RT (with a high-capacity cDNA archive kit) in a final volume of 50 μl. The reaction mixture consisted of 10× RT buffer (5 μl), 25× dNTP mixture (2 μl), 10× random primer (5 μl), 50 U/μl MultiScribe RT (2.5 μl), RNase inhibitor (2 μl), and nuclease-free water (8.5 μl). The mix was incubated at 25°C for 10 min and then at 37°C for 120 min and was then stored at −20°C until use.

Real-time PCR. Primers, which were designed using DNASTAR and synthesized by Bioneer, were as follows. Kir2.1 (GenBank accession no. AF021137): sense primer (328–351), 5′27-CAC GGG GAT CTG GAT GCT TCT AAA-3′; and antisense primer (448–471), 5′-AGC AAT CGG GCA CTC GTC TGT AAC-3′. Na^+-K^+ pump-α_1 (GenBank accession no. NM012504): sense primer (3252–3274), 5′-GAA GCT CAT CAT CAG GCG ACG-3′; and antisense primer (3390–3410), 5′-CCA GGG TAG AGT TCC GAG CTC-3′. Na^+-K^+ pump-α_2 (GenBank accession no. NM012505): sense primer (577–597), 5′-AGA ACA TGG TGC CTC AGC AAG-3′; and antisense primer (660–679), 5′-CCA CCC TTC ACT TCC ACC AG-3′. Na^+-K^+ pump-α_3 (GenBank accession no. NM012506): sense primer (3324–3345), 5′-CCA CAC CTC GGT TAC CTC TCA C-3′; and antisense primer (3508–3529), 5′-CAG ATT TAG AAC CGG AGA TGG C-3′. Real-time PCR was performed according to the recommendations of Applied Biosystems. SYBR green master mixes (2×; Applied Biosystems) were used to make the stock buffer. PCR was carried out in a 25-μl reaction mix that contained 20 ng of sample cDNA, primers, and 1× SYBR green universal PCR master mix (that contained $MgCl_2$, dUTP, dATP, dCTP, dGTP, AmpliTaq Gold polymerase, and AmpErase UNG). AmpErase UNG was activated before the denaturation step by heating for 2 min at 50°C. Samples were denatured at 95°C for 10 min and then subjected to 50 cycles of two-step PCR (15 s at 95°C, 1 min at 60°C) on an ABI Prism 7000 sequence detection system (Applied Biosystems). Samples were amplified simultaneously in triplicate in one assay run. Standard curves were computed for all genes from a series of fivefold serial template dilutions from 3.125–100 ng (five concentrations). For each sample, the amounts of each target gene and of β-actin (endogenous control) were determined from the corresponding standard curves.

Electrophysiology. Membrane potential was monitored in current-clamp mode with an EPC-9 amplifier (HEKA Elektronik; Lambrecht, Germany) using a nystatin-perforated patch (100 μg/ml). Whole cell currents were measured using ruptured patches. Voltages were monitored in voltage-clamp mode with an EPC-9 amplifier. The holding potential for the whole cell experiment was −60 mV. We applied a voltage ramp from −150 to +100 mV every 10 s with a duration of 650 ms. Currents were recorded at a sampling rate of 1–4 kHz.

The standard external solution contained (in mM) 150 NaCl, 6 KCl, 1.5 $CaCl_2$, 1 $MgCl_2$, 10 HEPES, and 10 glucose. The osmolarity of this solution as measured with a vapor-pressure osmometer (Fiske; Norwood, MA) was 320 ± 5 mosM. The standard pipette solution contained (in mM) 40 KCl, 100 potassium aspartate, 1 $MgCl_2$, 0.1 or 5 EGTA, 4 Na_2ATP, 10 HEPES, pH 7.2 with KOH (290 mosM).

Chemicals. Iberiotoxin, norepinephrine bitartrate (NE), ouabain, L-NAME, and tetraethylammonium chloride (TEA) were purchased from Sigma. Nystatin was purchased from ICN Biomedical and was applied from a stock solution in DMSO. The final concentration of DMSO was <0.05%.

Statistical analysis. Pooled data are presented as means ± SE. One-way ANOVA followed by the Turkey's test and repeated-measures ANOVA was used for multiple comparisons of pH_o-dependent changes of concentration-dependent responses to NE. In the other cases, statistical analysis was performed using Student's *t*-test. Values were considered statistically significant at $P < 0.05$.

RESULTS

Effects of pH_o on vascular contractility. In SMA branches and the trunk, NE induced concentration-dependent contractile responses. On decreasing pH_o from 7.8 to 6.4, NE-induced contraction was significantly reduced, and the concentration-response curves to NE were shifted to the right (Fig. 1, *A*-*D*). The pH_o-dependent changes of the contractions were more prominent in the trunk ($P < 0.001$; Fig. 1, *C* and *D*). In the second branch, pD_2 to NE was 5.38 ± 0.01 at pH_o 7.4. The pD_2 was increased to 5.44 ± 0.01 on increasing pH_o to 7.8 and reduced to 5.28 ± 0.01 and 5.17 ± 0.01 on decreasing pH_o to 6.9 and 6.4, respectively. In trunks, pD_2 was 5.66 ± 0.02 at pH 7.4, which was increased to 5.95 ± 0.02 on increasing pH_o to 7.8 and reduced to 5.47 ± 0.02 and 5.29 ± 0.02 on decreasing pH_o to 6.9 and 6.4, respectively. Concentration-dependent responses to NE and the pD_2 changes by pH_o of the first and

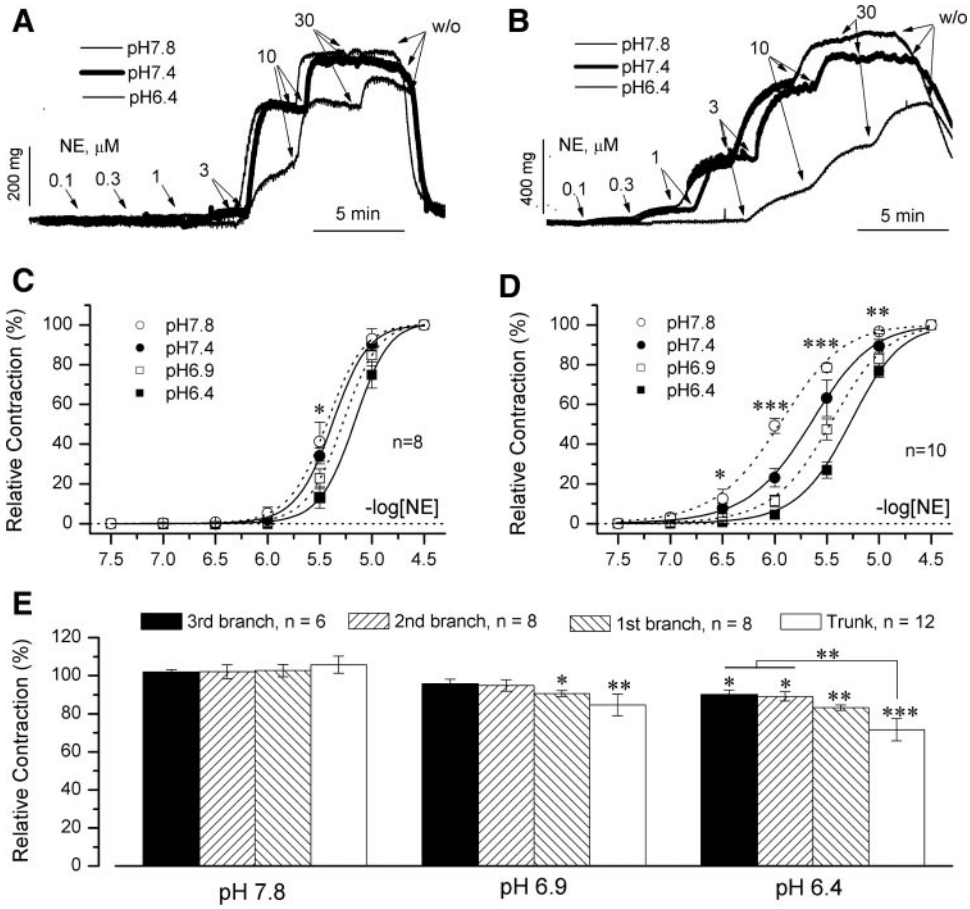

Fig. 1. Extracellular pH (pH_o)-dependent changes of vascular contractility in various diameter branches of rat superior mesenteric artery (SMA). Norepinephrine (NE) produced concentration-dependent contractions in SMA second branch (*A* and *C*) and trunk (*B* and *D*). Shift in concentration-response curve by changing pH_o was more pronounced in the trunk than in the second branch. Maximal contractions by 30 μM NE in SMA branches of various diameters are shown (*E*). Contractions at each pH_o were normalized vs. NE-induced contractions at pH 7.4. $^*P < 0.05$; $^{**}P < 0.01$; and $^{***}P < 0.001$. [NE], NE concentration.

the third branches were similar to those of the second branch (data not shown). In addition, maximal contraction by NE (30 μM) was also reduced on decreasing pH_o (Fig. 1*E*). Compared with contraction at pH_o 7.4, contractions of the third, second, and first branches and trunk were reduced to 89.98 ± 2.52, 89.13 ± 2.41, 83.28 ± 1.39, and 71.57 ± 5.79% on decreasing pH_o to 6.4, respectively. Thus pH_o-dependent pD_2 and NE-induced contraction changes were more prominent in trunks than in branches. These data suggest that the modulation of vascular contractility by H^+ depends on arterial diameters and that the decreases in vascular contractility by H^+ are more prominent in larger-diameter arteries.

Comparative characteristics between SMA branches and trunk. Precontracted arterial rings were relaxed on increasing $[K^+]_o$ from 6 to 12 mM (Fig. 2, *A* and *B*), and this relaxation is known as K^+-induced relaxation. We compared the magnitudes of K^+-induced relaxation in SMA branches and the trunk. As shown in Fig. 2*C*, K^+ evoked 92.66 ± 1.29, 60.34 ± 2.37, and 19.26 ± 1.35% relaxations in the third branch, the first branch, and the trunk, respectively. These results suggest that K^+-induced relaxation increases as the arterial diameter decreases.

Because Kir2.1 channels contribute K^+-induced relaxation (21), we examined the presence of Kir2.1 channels and compared the levels of their expression in SMA branches and the

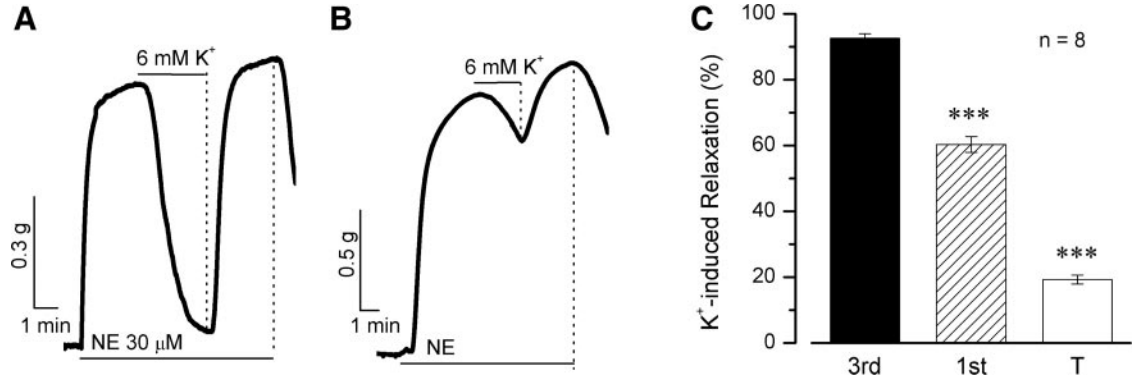

Fig. 2. K^+-induced relaxations in SMA branches of various diameters in the third branch (*A*) and trunk (*B*). Greatest K^+-induced relaxation was evoked in the smallest-diameter arteries (*A* and *C*). T, trunk. $^{***}P < 0.001$.

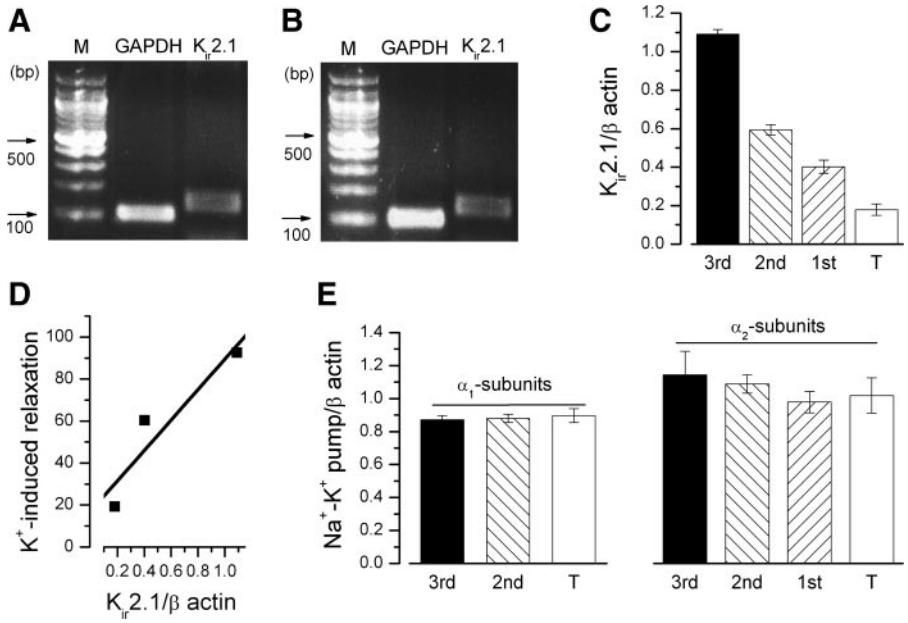

Fig. 3. Identification of Kir2.1 transcript by RT-PCR and quantitative analysis of transcripts of Kir2.1 and Na^+-K^+ pump α_1- and α_2-subunits by real-time PCR. *A* and *B*: identification of Kir2.1 in SMA branches (*A*) and trunk (*B*). Real-time PCR revealed that the Kir2.1 transcript level was higher in branches than in trunks (*C*). *C* and *D*: relation between transcript levels of Kir2.1 (*C*) and the magnitudes of K^+-induced relaxations (Fig. 2*C*) in SMA branches of various diameters (*D*). *E*: transcript levels of Na^+-K^+ pump α_1- and α_2-subunits by real-time PCR in SMA branches of various diameters.

trunk. We confirmed the presence of Kir2.1 transcripts in SMCs from SMA branches and the trunk by RT-PCR (Fig. 3, *A* and *B*), and significant differences in the transcript levels of Kir2.1 were found in branch and trunk SMCs (Fig. 3*C*). We observed 6.1-, 3.3-, and 2.2-fold increases in the Kir2.1 mRNA-to-β-actin mRNA ratios of SMCs of the third, second, and first branches, respectively, vs. the corresponding relative levels of trunk SMCs. There was a strong correlation between the transcript levels of Kir2.1 and K^+-induced relaxation (Fig. 3*D*). In contrast, no significant differences in the transcript levels of α_1- and α_2-subunits of the Na^+-K^+ pump were found in branch and trunk SMCs (Fig. 3*E*). In addition, no significant differences in the transcript levels of α_3-subunits of the Na^+-K^+ pump were found in branch and trunk SMCs (data not shown). These results suggest that K_{IR} channel densities increase with reduced arterial diameter, which accounts for the difference in the magnitude of K^+-induced relaxations between SMA branches and trunk.

Effects of pH_o on K^+-induced relaxation. In the first branch, K^+-induced relaxation of 63.94 ± 3.74% at pH 7.4 was increased to 95.09 ± 1.91% on increasing pH_o to 7.8 and reduced to 21.72 ± 1.89 and 9.72 ± 1.56% on decreasing pH_o to 6.9 and 6.4, respectively (Fig. 4). We then examined the effects of the K_{IR} channel blocker Ba^{2+} on K^+-induced relaxation. K^+-induced relaxations were completely inhibited by 30 μM Ba^{2+} at pH_o values of 6.4, 6.9, and 7.4 (Fig. 4, *A*-*C*). In contrast, K^+-induced relaxation at pH_o 7.8 was not inhibited by Ba^{2+} but was completely inhibited by Ba^{2+} with ouabain (Fig.

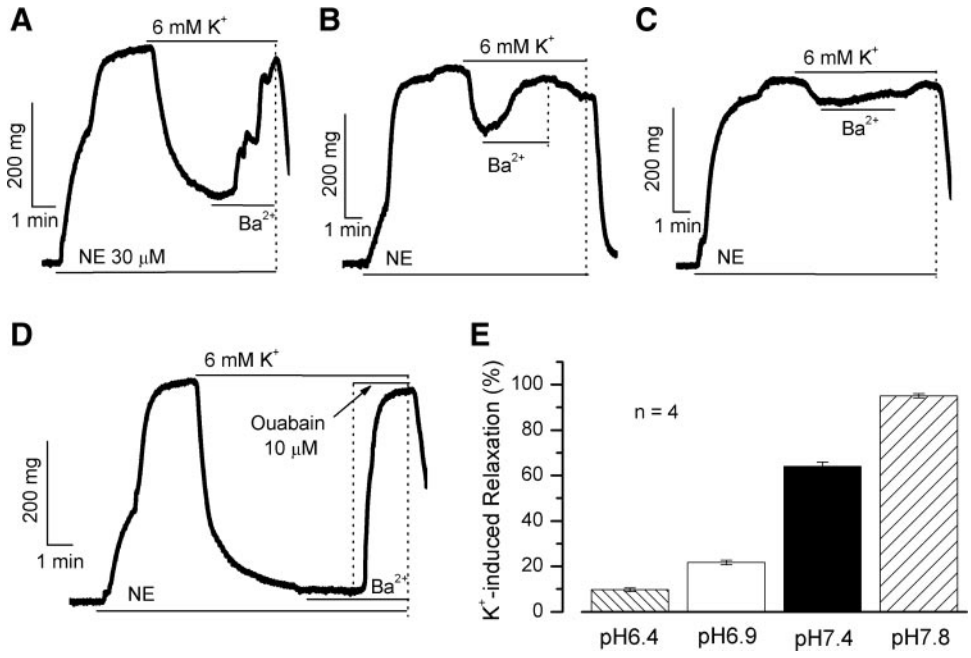

Fig. 4. Inhibition of K^+-induced relaxation by extracellular acidification in SMA first branch. NE-induced contractions were reduced on increasing extracellular K^+ concentration from 6 to 12 mM at pH_o 7.4, and relaxation was inhibited by Ba^{2+} (*A*). Ba^{2+}-sensitive K^+-induced relaxation was reduced at pH_o values of 6.9 (*B*) and 6.4 (*C*) and was increased at pH_o 7.8 (*D* and *E*).

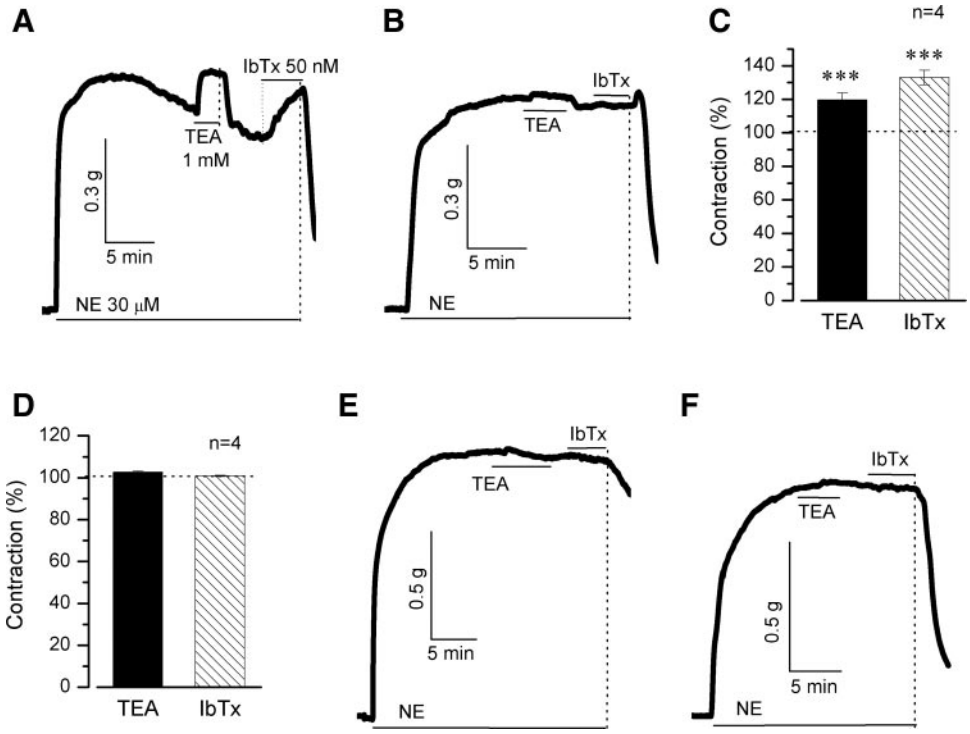

Fig. 5. Effects of the Ca^{2+}-activated K^+ channel blockers tetraethylammonium chloride (TEA) or iberiotoxin (IbTx) on NE-induced contraction. In the second branch, NE-induced contractions spontaneously decreased with time, and this decrease was reversed by TEA or IbTx at pH_o 7.4 (*A* and *C*). When pH_o was decreased to 6.4, contractions did not decrease with time and were unaffected by TEA or IbTx (*B* and *D*). In the trunk, TEA or IbTx caused no change in contraction at pH values of 7.4 and 6.4 (*E* and *F*). $***P < 0.001$.

4*D*). These findings suggest that an increase in pH_o activates Ba^{2+}- and ouabain-sensitive K^+-induced relaxation (Fig. 4, *D* and *E*). In addition, in HEPES-buffered solution, K^+-induced relaxation was inhibited on decreasing pH_o from 7.4 to 6.4 (data not shown).

During agonist-induced contraction, K^+ efflux occurs through large-conductance Ca^{2+}-activated K^+ channels in SMCs, and this can evoke K^+-induced relaxation that is sufficient to suppress the level of contraction by 75% (3). Thus we examined the effects of pH_o on the relaxation evoked by the released K^+ through large-conductance Ca^{2+}-activated K^+ channels during NE-induced contraction. In the second branch, in which K^+-induced relaxation is prominent, NE-induced contraction was spontaneously decreased with time, and this decrease was reversed by the Ca^{2+}-activated K^+ channel blockers TEA or iberiotoxin at pH_o 7.4 (Fig. 5, *A*and *C*). The decreasing tension was significantly increased to 119.62 ± 4.07 and 132.95 ± 4.31% on application of TEA or iberiotoxin, respectively (Fig. 5*C*). In contrast, in the trunk, in which K^+-induced relaxation is negligible, the spontaneous and TEA- or iberiotoxin-induced changes in contraction were not observed (Fig. 5*E*). These data suggest that K^+-induced relaxation might be evoked by the released K^+ through Ca^{2+}-activated K^+ channels during NE-induced contraction. The effects of pH_o on the relaxation was then examined. When pH_o was decreased to 6.4, NE-induced contraction was not spontaneously reduced, and no significant change in the contraction was detected on application of TEA or iberiotoxin in the second branch (Fig. 5, *B* and *D*) and trunk (Fig. 5*F*), although the release of K^+ through Ca^{2+}-activated K^+ channels might be increased because Ca^{2+}-activated K^+ channels are activated by acidification (4). These data also suggest that a decrease in pH_o inhibits K^+-induced relaxation.

Inwardly rectifying currents were recorded from cultured SMCs of SMA branches (Fig. 6). Because inwardly rectifying currents were found to be inhibited by 300 μM Ba^{2+} (Fig. 6, *A, B, D,* and *E*), these Ba^{2+}-sensitive currents may be K_{IR} currents. These Ba^{2+}-sensitive currents were significantly reduced on decreasing pH_o from 7.4 to 6.4 (Fig. 6, *A* and *C–E*). These results suggest that a decrease in pH_o inhibits K_{IR} channels.

Effects of pH_o on Na^+-K^+ pump. From the data shown in Fig. 4*D*, we suggested that an increase in pH_o activates the Na^+-K^+ pump. For further evaluations, we examined the effects of pH_o on Na^+-K^+ pump activity. Inasmuch as the relative contribution of the Na^+-K^+ pump to K^+-induced relaxation might be greater in larger-diameter arteries, the SMA trunk was used to examine ouabain-sensitive K^+-induced relaxation. Ouabain-sensitive K^+-induced relaxation was markedly reduced on decreasing pH_o from 7.4 to 6.4 (Fig. 7). K^+-induced relaxations of 17.74 ± 1.35% at pH_o 7.4 were reduced to 1.07 ± 0.26% on decreasing pH_o to 6.4. We then examined the effects of ouabain on resting tensions in SMA trunk. The resting tensions were not altered on pH_o changes. Then, ouabain was applied. On application of ouabain, the resting tensions were increased, and these increases were enhanced on increasing pH_o from 6.4 to 7.8 (Fig. 8). Compared with 10 μM NE-induced contraction at pH_o 7.4, ouabain increased the resting tension to 0.89 ± 0.89% at pH_o 6.4, whereas the tension was increased to 30.74 ± 1.78% at pH_o 7.8 (Fig. 8*E*). These findings suggest that ouabain-induced contraction decreases on acidification.

Effects of pH_o on membrane potential. The mean resting membrane potential of cultured SMCs from trunk was −55.56 ± 6.44 mV at pH_o 7.4 ($n = 8$), and this was significantly depolarized by −46.22 ± 6.63 mV on decreasing pH_o to 6.4 (Fig. 9, *A* and *B*). Ouabain depolarized membrane potential at pH_o 7.4 (Fig. 9*C*), whereas membrane potential was unaffected by ouabain treatment at pH_o 6.4 (Fig. 9*D*). These

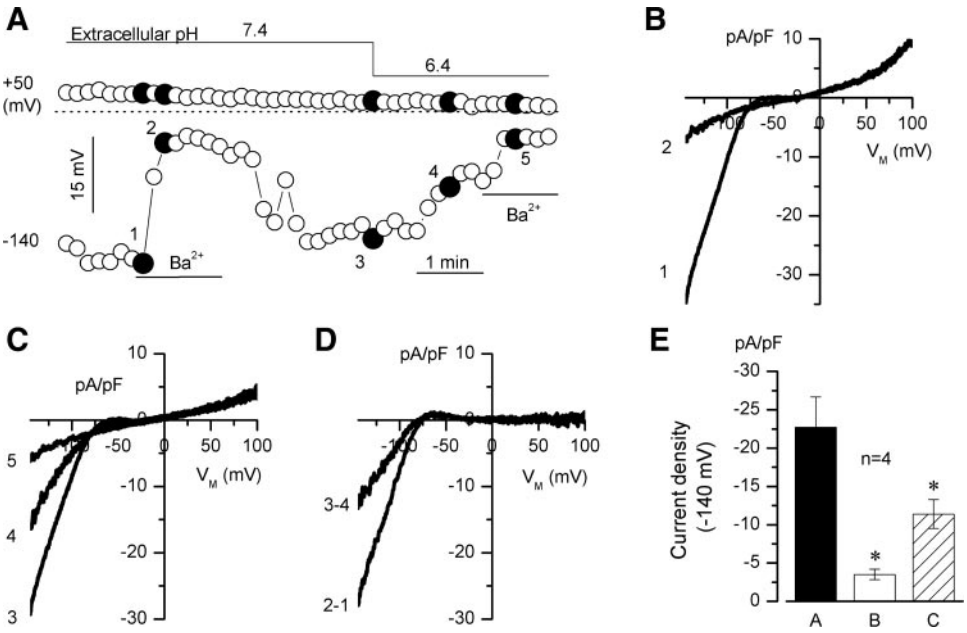

Fig. 6. Inhibition of inwardly rectifying K^+ (K_{IR}) currents by extracellular acidification. Time course of the membrane currents is shown (*A*). Data points were obtained at 50 and −140 mV during repetitive ramps from −150 to +100 mV. Current-voltage (*I-V*) relations were obtained at the points marked in *A* (*B* and *C*). Difference currents before and after application of Ba^{2+} (2–1) or decreasing pH_o from 7.4 to 6.4 (3–4) are shown (*D*). Inwardly rectifying currents were inhibited by Ba^{2+} (*B* and *D*) and by extracellular acidification (*C* and *D*). Current density, measured at −140 mV (*E*), was significantly reduced by Ba^{2+} or extracellular acidification. V_M, membrane voltage. $^*P < 0.05$.

findings suggest that ouabain-induced depolarization decreases on acidification.

DISCUSSION

This study provides evidence to indicate that the Na^+-K^+ pump and K_{IR} channels participate in the pH_o-dependent control of vascular contractility. The results of the present study indicate that *1*) an increase in pH_o potentiates vascular contractility; *2*) the pH_o-dependent control of vascular contractility is more prominent in larger-diameter arteries, on the contrary; *3*) a decrease in pH_o inhibits K_{IR} currents; *4*) K_{IR} channel densities are significantly greater in the SMCs of smaller-diameter branches than in those of larger-diameter branches; and *5*) an increase in pH_o potentiates, and a decrease in pH_o inhibits, the Na^+-K^+ pump activity. From these results, we conclude that extracellular alkalinization activates K_{IR} channels and the Na^+-K^+ pump, which in turn reduces vascular contractility and thereby attenuates the increased vascular contractility induced by extracellular alkalinization. Inasmuch as K_{IR} channel densities are significantly greater in smaller-diameter than in larger-diameter arteries, the attenuation is more pronounced in smaller-diameter arteries.

K^+-induced relaxation is evoked via the Na^+-K^+ pump and K_{IR} channel activation (11, 21). K_{IR} channel conductance, which is dependent on membrane potential, is very small at potential positive to the calculated equilibrium potential for K^+ (E_K) and starts to increase as membrane potential hyperpolarizes to $\sim E_K$. When SMA is contracted by NE (30 μM), membrane potential may depolarize because the resting membrane potential of rat SMA was approximately −60 mV and depolarized to approximately −40 mV by phenylephrine (10 μM) (19). Inasmuch as E_K at 6 mM $[K^+]_o$ is approximately −85 mV (150 mM $[K^+]_i$ and 37°C), the conductance of K_{IR} channels may be negligible during NE-induced contraction. On $[K^+]_o$ elevation in a millimolar range, E_K is shifted to the more positive potential (the calculated E_K is approximately −65 mV at 12 mM $[K^+]_o$), and the conductance of K_{IR} channels increases. In addition, $[K^+]_o$ elevation activates the Na^+-K^+

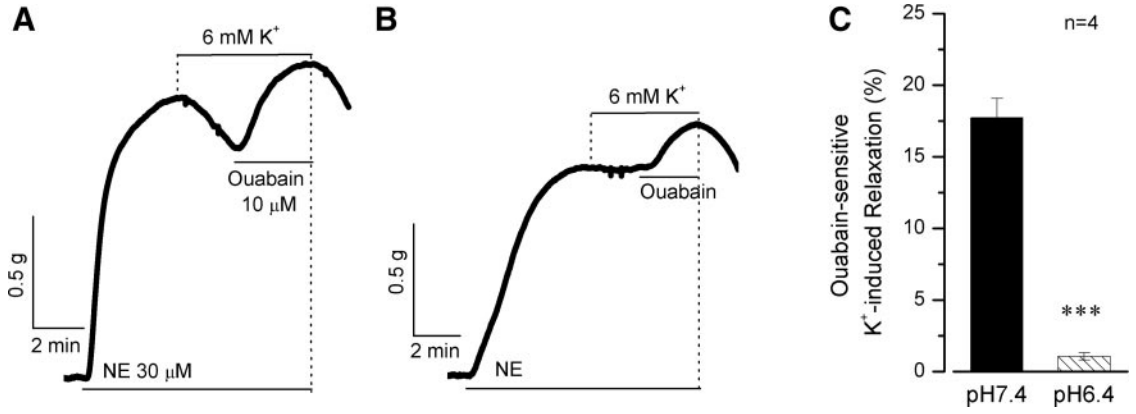

Fig. 7. Effects of extracellular acidification on ouabain-sensitive K^+-induced relaxation. Tracings show responses to pH_o values of 7.4 (*A*) and 6.4 (*B*). In SMA trunk, K^+-induced relaxation was inhibited by ouabain (a Na^+-K^+ pump inhibitor), and ouabain-sensitive relaxation was reduced by extracellular acidification (*C*). $^{***}P < 0.001$.

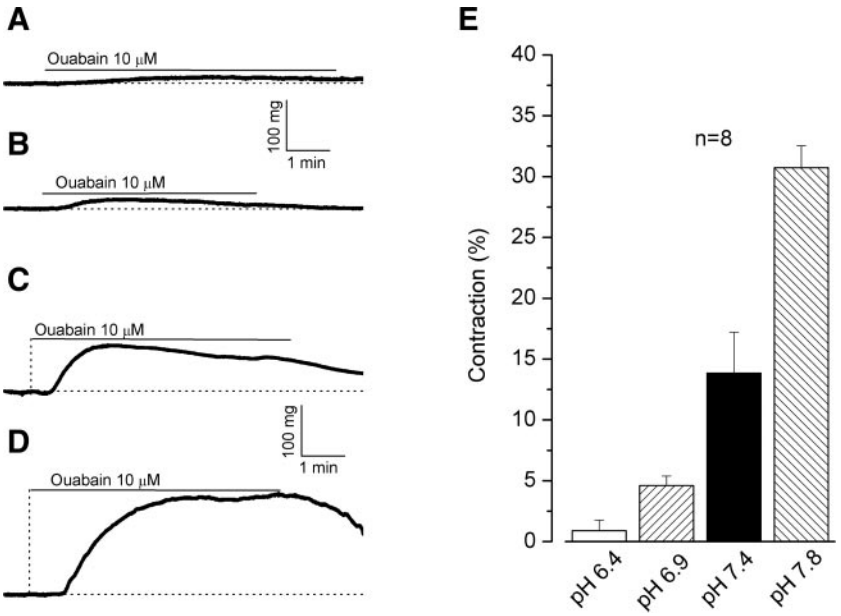

Fig. 8. Effects of pH_o on ouabain-induced contractions in SMA trunks. Ouabain-induced contractions of trunk were significantly enhanced on increasing pH_o values from 6.4 (*A*) to 6.9 (*B*), 7.4 (*C*), and 7.8 (*D*). Magnitudes of the contractions were expressed as a percentage of 10 μM NE-induced contraction at pH_o 7.4 (*E*).

pump. K_{IR} channel conductance increase and Na^+-K^+ pump activation hyperpolarize membrane potential. This hyperpolarization inhibits voltage-gated Ca^{2+} channels and relaxes the vascular smooth muscle. In contrast, vascular smooth muscle contracts in response to $[K^+]_o$ elevation to >25 mM. Thus 12 or 15 mM K^+ may be enough to evoke K^+-induced relaxation (8, 21). Among the Na^+-K^+ pump and K_{IR} channels, K_{IR} channels may be a main contributor in K^+-induced relaxation, because Kir2.1 gene expression in arterial smooth muscle is required for K^+-induced relaxation (21).

Role of K_{IR} channels in pH_o-dependent control of vascular contractility. The magnitude of K^+-induced relaxation varies depending on arterial diameter; the relaxation is prominent in small-diameter arteries such as resistant arteries and SMA branches, whereas it is relatively small or negligible in large-diameter arteries such as the SMA trunk. Kir2.1 gene expression in arterial SMCs is required for K_{IR} currents and K^+-induced relaxation (21). Real-time PCR analysis revealed significant differences in Kir2.1 transcript levels in SMA branches and trunks, and the smallest-diameter branch showed the highest Kir transcript expression. In addition, the magnitude of K^+-induced relaxation was greater in smaller-diameter branches. These findings suggest that K_{IR} channel densities are higher in smaller-diameter arteries, which is consistent with previous work (2, 15). The highest Kir2.1 transcript levels were found in SMCs from the smallest-diameter artery in the rat (2), and K_{IR} current densities were higher in SMCs from smaller-diameter porcine coronary arteries (15).

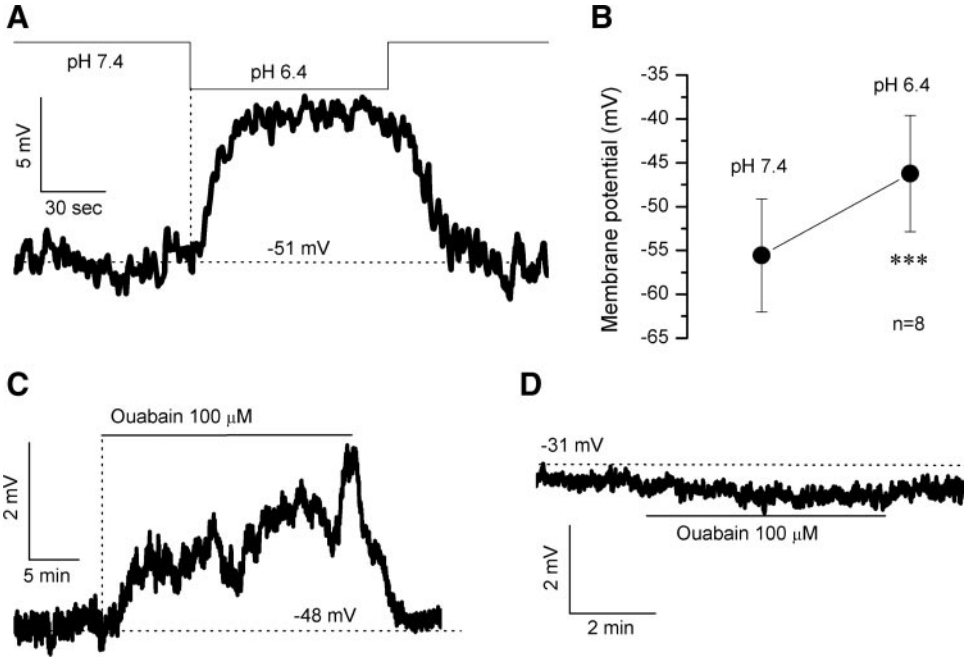

Fig. 9. Effects of pH_o and ouabain on membrane potential of cultured smooth muscle cells from SMA trunk. A decrease in pH_o from 7.4 to 6.4 (*A* and *B*) or treatment with ouabain at pH_o values of 7.4 (*C*) and 6.6 (*D*) significantly depolarized resting membrane potentials. $***P < 0.001$.

In SMA branches and trunks, differences in K_{IR} channel densities may have caused the observed differences in pH_o-dependent changes in vascular contractility (see Fig. 1). In agreement with previous studies (22), the present study showed that a decrease in pH_o inhibited K_{IR} currents. A decrease in pH_o inhibits K_{IR} currents by affecting mainly single channel conductance (2). They showed that Kir2.3 current inhibition by extracellular acidification started at pH 7.0 and plateaued at pH 6.0 with a pK of 6.7. Our finding that Ba^{2+}-sensitive K^+-induced relaxation was markedly reduced at pH_o values of 6.9 and 6.4 is consistent with this finding. K_{IR} current activation would be expected to lead to hyperpolarization and hence, to relaxation. Thus when pH_o is increased, K_{IR} current activation would be expected to attenuate the increase of vascular contractility. Inasmuch as the channel densities are higher in SMCs of smaller-diameter arteries, the attenuation may be more prominent in smaller-diameter arteries, and therefore the pH_o-dependent changes in pD_2 and NE-induced contractions were less pronounced in smaller-diameter arteries.

Cell phenotype may change during cell culture. However, it is unlikely that the recorded K_{IR} current is a culture artifact for a couple of reason. First, transcript for Kir2.1 was also detected in freshly isolated cells from rat SMA (2). Thus transcript for Kir2.1 is detected not only in cultured SMCs but also in freshly isolated cells. Second, K^+-induced relaxation was inhibited by Ba^{2+}. This suggests that K_{IR} channel contributes K^+-induced relaxation in rat SMAs. In addition, there was a strong correlation between the transcript levels of Kir2.1 and the magnitude of K^+-induced relaxation. These results suggest the presence of K_{IR} channels and a functional role for K_{IR} channels to evoke K^+-induced relaxation in rat SMAs.

Role of Na^+-K^+ pump in pH_o-dependent control of vascular contractility. The contribution of K_{IR} channels to K^+-induced relaxation would depend on K_{IR} channel densities and thus would be greater in smaller-diameter arteries. On the contrary, no significant differences in the Na^+-K^+ pump densities were found in SMA branches and the trunk. Therefore, we suggest that Na^+-K^+ pump expression is independent of arterial diameter and that the relative contribution of the Na^+-K^+ pump to K^+-induced relaxation may be greater in larger-diameter arteries.

Acidification depolarized the membrane potential of cultured SMCs from the SMA trunk, which is consistent with previous findings (13, 14). They showed that normocapnic acidosis caused depolarization in intact arteries of the rat. However, they did not examine the mechanism of acidification-induced depolarization. In this study, we suggest that acidification-induced depolarization is evoked by inhibition of the Na^+-K^+ pump and K_{IR} channel. Compared with the Na^+-K^+ pump, the contribution of K_{IR} channels to acidification-induced depolarization may be relatively small in the resting or agonist-stimulated conditions, because the membrane potential of SMCs is positive to the E_K in both conditions.

Ouabain depolarizes membrane potential by inhibiting the Na^+-K^+ pump. Inasmuch as depolarization may evoke contraction by increasing Ca^{2+} influx through VOC channels, ouabain-induced contraction might be at least in part evoked by ouabain-induced depolarization. In contrast, a decrease in pH_o, which also depolarized membrane potential, did not evoke contraction. This absence of acidification-induced contraction can be clearly explained by a previous report showing that acidification inhibits VOC channels (6, 7). This effect of H^+ on VOC channels can also explain why ouabain-induced contractions decrease on acidification. In addition, inasmuch as ouabain did not induce depolarization at pH_o 6.4, we suggest that ouabain-induced depolarization is decreased on acidification and that the decrease in ouabain-induced depolarization contributes to a decrease in ouabain-induced contraction on acidification.

Na^+-K^+ pump expression and activity is regulated by a variety of moieties that include the cytoskeleton, endogenous inhibitors, and protein kinases (18). Membrane potential also affects Na^+-K^+ pump activity. Depolarization would increase the amplitude of the Na^+-K^+ pump currents, because membrane potential moves further from the reversal potential (12). However, when pH_o was decreased to 6.4, ouabain failed to evoke depolarization, because H^+ inhibits the Na^+-K^+ pump. The mechanism of Na^+-K^+ pump inhibition by H^+ remains to be investigated.

Physiological implications. Here, we propose that the Na^+-K^+ pump and K_{IR} channels play important roles in pH_o-dependent control of vascular contractility in smaller diameter arteries. Acidification decreases Ca^{2+} influx through VOC channels and Ca^{2+} sensitivity of contractile proteins (9) in SMCs and thus decreases vascular contractility. On the contrary, acidification inhibits the Na^+-K^+ pump and K_{IR} channels, and vascular contractility can be increased by the inhibition. Therefore, the Na^+-K^+ pump and K_{IR} channels may inhibit excessive changes in vascular contractility by pH and sensitively control blood flow. In pathological conditions such as hypoxia, pH_o decreases. Hence K_{IR} channel inhibition is likely to impact on the extent of blood flow increases under hypoxic conditions and appears to be an important negative-feedback process that limits blood flow increases.

The results of the present study show that rat mesenteric artery SMCs possess Kir2.1 channels that evoke K^+-induced relaxation, and the channel expression increases as arterial diameter decreases. Furthermore, we show that an increase in pH_o potentiates and a decrease in pH_o inhibits K_{IR} currents and Na^+-K^+ pump activity. Thus the increase of vascular contractility by extracellular alkalinization is more pronounced in larger-diameter arteries.

GRANTS

This work was supported by the Advanced Backbone IT Technology Development Project from the Ministry of Information and Communication (IMT2000-C3-3).

REFERENCES

1. **Austin C and Wray S.** Interactions between Ca^{2+} and H^+ and functional consequences in vascular smooth muscle. *Circ Res* 86: 355–363, 2000.
2. **Bradley KK, Jaggar JH, Bonev AD, Heppner TJ, Flynn ER, Nelson MT, and Horowitz B.** Kir2.1 encodes the inward rectifier K^+ channel in rat arterial smooth muscle cells. *J Physiol* 515: 639–651, 1999.
3. **Dora KA, Hinton JM, Walker SD, and Garland CJ.** An indirect influence of phenylephrine on the release of endothelium-derived vasodilators in rat small mesenteric artery. *Br J Pharmacol* 129: 381–387, 2000.
4. **Hayabuchi Y, Nakaya Y, Matsuoka S, and Kuroda Y.** Effect of acidosis on Ca^{2+}-activated K^+ channels in cultured porcine coronary artery smooth muscle cells. *Pflügers Arch* 436: 509–514, 1998.
5. **Horiuchi T, Dietrich HH, Hongo K, Goto T, and Dacey RG Jr.** Role of endothelial nitric oxide and smooth muscle K^+ channels in cerebral arteriolar dilation in response to acidosis. *Stroke* 33: 844–849, 2002.
6. **Klockner U and Isenberg G.** Ca^{2+} channel current of vascular smooth muscle cells: extracellular protons modulate gating and single channel conductance. *J Gen Physiol* 103: 665–678, 1994.

7. **Klockner U and Isenberg G.** Intracellular pH modulates the availability of vascular L-type Ca^{2+} channels. *J Gen Physiol* 103: 647–663, 1994.
8. **Knot HJ, Zimmermann PA, and Nelson MT.** Extracellular K^+-induced hyperpolarizations and dilatations of rat coronary and cerebral arteries involve inward rectifier K^+ channels. *J Physiol* 492: 419–430, 1996.
9. **Komukai K, Ishikawa T, and Kurihara S.** Effects of acidosis on Ca^{2+} sensitivity of contractile elements in intact ferret myocardium. *Am J Physiol Heart Circ Physiol* 274: H147–H154, 1998.
10. **Mao J, Wu J, Chen F, Wang X, and Jiang C.** Inhibition of G-protein-coupled inward rectifying K^+ channels by intracellular acidosis. *J Biol Chem* 278: 7091–7098, 2003.
11. **McCarron JG and Halpern W.** K^+ dilates rat cerebral arteries by two independent mechanisms. *Am J Physiol Heart Circ Physiol* 259: H902–H908, 1990.
12. **Nakamura Y, Ohya Y, Abe I, and Fujishima M.** Na^+-K^+ pump current in smooth muscle cells from mesenteric resistance arteries of the guinea-pig. *J Physiol* 519: 203–212, 1999.
13. **Peng HL, Ivarsen A, Nilsson H, and Aalkjaer C.** On the cellular mechanism for the effect of acidosis on vascular tone. *Acta Physiol Scand* 164: 517–525, 1998.
14. **Peng HL, Jensen PE, Nilsson H, and Aalkjaer C.** Effect of acidosis on tension and $[Ca^{2+}]_i$ in rat cerebral arteries: is there a role for membrane potential? *Am J Physiol Heart Circ Physiol* 274: H655–H662, 1998.
15. **Quayle JM, Dart C, and Standen NB.** The properties and distribution of inward rectifier K^+ currents in pig coronary arterial smooth muscle. *J Physiol* 494: 715–726, 1996.
16. **Robertson BE, Bonev AD, and Nelson MT.** Inward rectifier K^+ currents in smooth muscle cells from rat coronary arteries: block by Mg^{2+}, Ca^{2+}, and Ba^{2+}. *Am J Physiol Heart Circ Physiol* 271: H696–H705, 1996.
17. **Schubert R, Lehmann G, Serebryakov VN, Mewes H, and Hopp HH.** cAMP-dependent protein kinase is in an active state in rat small arteries possessing a myogenic tone. *Am J Physiol Heart Circ Physiol* 277: H1145–H1155, 1999.
18. **Therien AG and Blostein R.** Mechanisms of Na^+ pump regulation. *Am J Physiol Cell Physiol* 279: C541–C566, 2000.
19. **Weston AH, Richards GR, Burnham MP, Feletou M, Vanhoutte PM, and Edwards G.** K^+-induced hyperpolarization in rat mesenteric artery: identification, localization and role of Na^+/K^+-ATPases. *Br J Pharmacol* 136: 918–926, 2002.
20. **Xu H, Cui N, Yang Z, Qu Z, and Jiang C.** Modulation of $K_{ir}4.1$ and $K_{ir}5.1$ by hypercapnia and intracellular acidosis. *J Physiol* 524: 725–735, 2000.
21. **Zaritsky JJ, Eckman DM, Wellman GC, Nelson MT, and Schwarz TL.** Targeted disruption of $K_{ir}2.1$ and $K_{ir}22$ genes reveals the essential role of the inwardly rectifying K^+ current in K^+-mediated vasodilation. *Circ Res* 87: 160–166, 2000.
22. **Zhu G, Chanchevalap S, Cui N, and Jiang C.** Effects of intra- and extracellular acidifications on single channel $K_{ir}2.3$ currents. *J Physiol* 516: 699–710, 1999.